# Synthesizing arbitrary two-photon polarization mixed states

Tzu-Chieh Wei,[1] Joseph B. Altepeter,[1] David Branning*,[1] Paul M. Goldbart,[1] D. F. V. James,[2] Evan Jeffrey,[1] Paul G. Kwiat,[1] Swagatam Mukhopadhyay,[1] and Nicholas A. Peters[1]

[1] *Department of Physics, University of Illinois at Urbana-Champaign, Urbana, Illinois 61801-3080*
[2] *Theoretical Division, T-4, Los Alamos National Laboratory, Los Alamos, New Mexico 87545*

(Dated: November 23, 2004)

Two methods for creating arbitrary two-photon polarization *pure* states are introduced. Based on these, four schemes for creating two-photon polarization *mixed* states are proposed and analyzed. The first two schemes can synthesize completely arbitrary two-qubit mixed states, i.e., control all 15 free parameters: Scheme I requires several sets of crystals, while Scheme II requires only a single set, but relies on decohering the pump beam. Additionally, we describe two further schemes which are much easier to implement. Although the total capability of these is still being studied, we show that they can synthesize all two-qubit Werner states, maximally entangled mixed states, Collins-Gisin states, and arbitrary Bell-diagonal states.

PACS numbers: 03.67.Mn, 42.50.Dv, 42.65.Lm

## I. INTRODUCTION

Quantum information processing [1] promises great power relative to its classical counterpart. Many quantum information processes require specific pure entangled states, such as Bell states, to succeed. After interacting with the environment, however, pure states inevitably decohere; decoherence generally causes pure entangled states to become mixed and less entangled. Quantum error correction [2] and entanglement distillation/concentration [3] have been developed to help cope with a noisy (and hence decohering) environment. On the other hand, there are implementations using mixed states to investigate quantum computing, e.g., liquid-state NMR [4]. The states in this last example are highly mixed and have no entanglement. Still, between highly entangled pure states and highly separable mixed states there exists a vast experimentally unexplored region in Hilbert space (more precisely, the space of density matrices), where states can be simultaneously mixed and entangled. The two-qubit system possesses the simplest and smallest Hilbert space that permits the existence of entanglement. Separate from the specific protocols which make use of the states, it is of fundamental interest to understand the preparation of one of the most basic quantum systems. Although there have been many attempts [5–8] to synthesize two-qubit mixed polarization states, none has yet been able to create completely arbitrary two-qubit mixed states [9].

Here we describe several two-photon polarization state implementations that should in principle enable preparation of arbitrary two-qubit mixed states, including states possessing all physical degrees of entanglement and entropy. The schemes we shall present facilitate state creation and allow access to two-qubit Hilbert space and can be useful for current and future quantum information protocols. We remark that if there exist efficient two-qubit entangling gates such as CNOT [1], arbitrary state synthesis can be systematically implemented by first generating a purification [10] of the mixed state by adding ancillas, and then tracing over the ancillas. However, efficient photon-polarization CNOT gates do not exist [11], so we rely on other degrees of freedom to introduce decoherence, leading to mixed states.

The paper is organized as follows. After a brief background discussion in Sec. I A, we describe, in Sec. II, two schemes to achieve *arbitrary pure* two-photon polarization states by employing downconversion in a two-crystal arrangement. The first one is based on the existence of Schmidt decompositions. The second one utilizes the coherent superpositions of two downconversion processes embedded in an interferometric setup. In Sec. III we describe how to extend these two schemes to realize arbitrary two-qubit *mixed* states (Schemes I and II). In Sec. IV we propose two reduced schemes (III and IV) that provide practical ways to realize several important families of states that are currently of interest, including Werner states [12], maximally entangled mixed states [13], Collins-Gisin states [14], and arbitrary Bell-diagonal states. Scheme III requires only two downconversion crystals, but cannot synthesize all two-qubit states. Scheme IV partially extends the set of attainable states, but requires four downconversion crystals. Finally, in Sec. V we summarize the four schemes and mention possible applications. Readers who do not require full details but want an overview of the four schemes and synthesizable states can refer to Table I. The details of how to create particular families of states can be found around the equations [(16), (19), (23), and (29)] describing these states.

*Present address: Department of Physics and Optical Engineering, Rose-Hulman Institute of Technology, Terre Haute, IN 47803, USA.

### A. Background information

The entangled photon pairs we consider come from frequency-degenerate type-I spontaneous parametric downconversion (SPDC) [15]. The general state from SPDC is a two-mode squeezed state consisting of vacuum and $k$-pair states [16]:

$$|\Psi\rangle = |\text{vacuum}\rangle + \varepsilon|\psi^{(1)}\rangle + \varepsilon^2|\psi^{(2)}\rangle + \cdots, \qquad (1)$$

where $|\psi^{(k)}\rangle$ is a $k$-pair state, and $\varepsilon$ is the relative amplitude (typically of order $10^{-6}$) to find a single pair. The post-selected 1-pair state $|\psi^{(1)}\rangle$ is composed of two daughter photons, usually called *signal* and *idler*. For the present article, we limit our attention to the case where the signal and idler photons have approximately degenerate central frequencies, half that of the pump. (Our schemes apply to nondegenerate case as well.) When the downconversion momenta are well collimated or otherwise sharply selected (experimentally by a small iris), one can neglect the momentum dependence of the pair state. The post-selected two-photon state can then be described by

$$|\psi^{(1)}(\omega)\rangle = \underbrace{\Big\{\sum_{j,k} c_{jk}|\chi_j,\chi_k\rangle\Big\}}_{\text{polarization}} \otimes \underbrace{\int d\epsilon\, A_{si}(\epsilon)\,|\tfrac{\omega}{2}+\epsilon, \tfrac{\omega}{2}-\epsilon\rangle}_{\text{frequency}}, \qquad (2)$$

where $\omega$ is the pump frequency. $|\chi_j,\chi_k\rangle$ and $|\frac{\omega}{2}+\epsilon, \frac{\omega}{2}-\epsilon\rangle$ respectively represent the polarizations and frequencies of the two photons, with $|\chi_1\rangle \equiv |H\rangle$, the horizontal polarization, and $|\chi_2\rangle \equiv |V\rangle$, the vertical polarization. $c_{jk}$ is the amplitude of the polarization state $|\chi_j,\chi_k\rangle$; for single-crystal type-I phase-matching the polarization state is unentangled, i.e., $c_{jk} = a_j b_k$. $A_{si}(\epsilon)$ is the amplitude for a particular division of energy, so that $\epsilon$ indicates the deviation from half pump frequency. $|A_{si}(\epsilon)|^2$ is peaked at $\epsilon = 0$ with width $\delta_\epsilon$, and we shall approximate it by a gaussian distribution:

$$|A_{si}(\epsilon)|^2 = \frac{1}{\sqrt{2\pi\delta_\epsilon^2}} \exp\left(-\frac{\epsilon^2}{2\delta_\epsilon^2}\right). \qquad (3)$$

More generally, the pump is not monochromatic, and therefore the pair state should be described by

$$|\psi\rangle = \int d\omega A_p(\omega)|\psi^{(1)}(\omega)\rangle, \qquad (4)$$

where $A_p(\omega)$ describes the frequency spread of the pump, assumed to be peaked at some frequency $\omega_0$ with half-width $\delta_\omega$. For most of the following discussion, we consider thicknesses of waveplates and crystals that are much less than the coherence length $l_p$ ($\equiv c/\delta_\omega$) of the pump, and hence we can safely use Eq. (2). The coherence length of downconversion photons ($l_{si} \equiv c/\delta_\epsilon$) is usually much smaller than $l_p$, i.e., $c/\delta_\epsilon \ll c/\delta_\omega$, because there are many ways to distribute the energy of the pump photon between the daughter photons in each pair, resulting in a large $\delta_\epsilon$ [17].

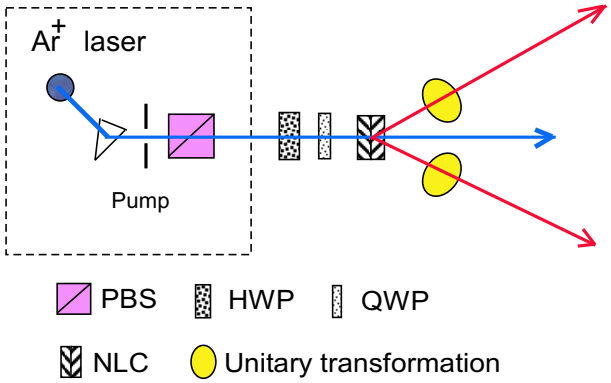


FIG. 1: (Color online) Arbitrary pure states via Schmidt decomposition. PBS: polarizing beam splitter; HWP: half-waveplate; QWP: quarter-waveplate; NLC: nonlinear crystals.

## II. SCHEMES FOR ARBITRARY TWO-PHOTON POLARIZATION PURE STATES

### A. Via Schmidt decomposition

Using the method of Schmidt decomposition [1], an arbitrary two-qubit pure state $|\psi\rangle = a|HH\rangle + b|HV\rangle + c|VH\rangle + d|VV\rangle$ can always be written using only two terms:$|\psi\rangle = \alpha|\chi\xi\rangle + \beta|\chi^\perp\xi^\perp\rangle$, where $|\chi\rangle$ ($|\xi\rangle$) is orthogonal to $|\chi^\perp\rangle$ ($|\xi^\perp\rangle$), and $\alpha$ and $\beta$ satisfy $|\alpha|^2 + |\beta|^2 = 1$.

Now we describe how to prepare such a state. The creation of the entangled state

$$\cos\theta|H_A H_B\rangle + e^{i\phi}\sin\theta|V_A V_B\rangle \qquad (5)$$

from two-crystal downconversion was proposed in Ref. [15]. Consider two identically cut thin nonlinear crystals. Suppose the first crystal's optic axis lies in the vertical plane defined by the directions of pump beam and the vertical polarization. Assuming type-I phase matching, a $V$-polarized pump will produce two $H$-polarized daughter photons. We denote this process by $|V\rangle \to |H_A\rangle \otimes |H_B\rangle$. If the pump is $H$-polarized, no downconversion process will take place. Suppose the second crystal is placed at an orientation rotated from the first crystal by 90° about the pump direction. An $H$-polarized pump will now produce a pair of $V$-polarized photons $|H\rangle \to |V_A\rangle \otimes |V_B\rangle$, whereas no downconversion will occur if the pump is $V$-polarized [18]. With the two crystals placed in contact with each other, a pump in the state $\cos\theta|V\rangle + e^{i\phi}\sin\theta|H\rangle$ will produce a pair of photons in the state

$$\cos\theta|H_A H_B\rangle + e^{i\phi}\sin\theta|V_A V_B\rangle,$$

where $\theta$ and $\phi$ are tuned using waveplates acting on the pump polarization [15]. ($\phi$ can also be tuned with, e.g., a variable waveplate acting on just one of the downconversion photons.)

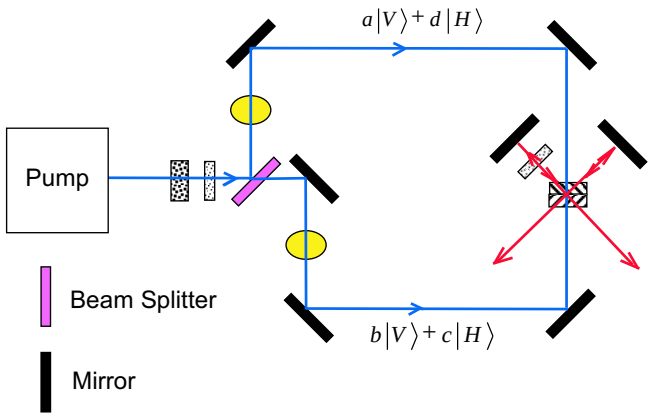


FIG. 2: (Color online) Arbitrary pure states via inteferometry.

Choosing the local unitary transformations $\hat{U}_A$ and $\hat{U}_B$ such that

$$\hat{U}_A\{|H\rangle, |V\rangle\} \rightarrow \{|\chi\rangle, |\chi^\perp\rangle\}, \quad (6a)$$
$$\hat{U}_B\{|H\rangle, |V\rangle\} \rightarrow \{|\xi\rangle, |\xi^\perp\rangle\}, \quad (6b)$$

we can achieve the arbitrary two-qubit pure state $|\psi\rangle$ by starting with an entangled state with $(\cos\theta, e^{i\phi}\sin\theta) = (\alpha, \beta)$ [up to an irrelevant overall phase], followed by the corresponding local rotations $\hat{U}_A$ and $\hat{U}_B$

$$\begin{aligned}&\hat{U}_A \otimes \hat{U}_B\big(\cos\theta|H_A H_B\rangle + e^{i\phi}\sin\theta|V_A V_B\rangle\big)\\ &= a|H_A H_B\rangle + b|H_A V_B\rangle + c|V_A H_B\rangle + d|V_A V_B\rangle. \quad (7)\end{aligned}$$

The two rotations can be obtained in the process of Schmidt decomposing $|\psi\rangle$ [1]; see also Appendix A for an explicit construction of the appropriate $\hat{U}$'s, $\alpha$, and $\beta$ given $\{a, b, c, d\}$.

In practice, any $SU(2)$ rotation such as $\hat{U}_A$ and $\hat{U}_B$ on a polarization state can be implemented by combinations of half- and quarter-waveplates [19]—preferably zero-order waveplates [20], for which the retardance is barely sensitive to deviation from the central frequency. That is to say, the action of waveplates, $\hat{U}$, can be assumed to be $\epsilon$-independent (at least in the frequency range set by the interference filter before detection), i.e.,

$$\hat{U}\{|\chi_j\rangle \otimes \int d\epsilon A(\epsilon)|\frac{\omega}{2} \pm \epsilon\rangle\} \approx \sum_k U_{kj}|\chi_k\rangle \otimes \int d\epsilon A(\epsilon)|\frac{\omega}{2} \pm \epsilon\rangle, \quad (8)$$

where $U_{kj}$ are the elements of a unitary matrix that is independent of $\epsilon$. We shall assume throughout this paper that unitary transformations by waveplates are ideal and independent of deviation from the central frequency.

### B. Via interferometry

A second method for creating arbitrary pure states is shown in Fig. 2 and is a modification from the setup of Ref. [21]. As discussed in Sec. II, via SPDC (assuming type-I phase matching), a pump in a polarization state $\alpha|H\rangle + \beta|V\rangle$ will generate an entangled photon pair in the state (up to some irrelevant phases) $\alpha|VV\rangle + \beta|HH\rangle$. With a half-waveplate, this entangled state can be further transformed into $\alpha|VH\rangle + \beta|HV\rangle$. Now, an arbitrary pure two-photon polarization state $a|HH\rangle + b|HV\rangle + c|VH\rangle + d|VV\rangle$ can be regarded as a superposition of two (un-normalized) parts: $a|HH\rangle + d|VV\rangle$ and $b|HV\rangle + c|VH\rangle$. The first part can be created from the (un-normalized) pump state $|\psi_U\rangle \equiv a|V\rangle + d|H\rangle$. To create the second part, we need the (un-normalized) pump state $|\psi_L\rangle \equiv b|V\rangle + c|H\rangle$, from which SPDC yields the two-photon state $b|HH\rangle + c|VV\rangle$. Again, a half-waveplate in one arm (or equivalently, passing through a quarter-waveplate twice) can transform this state into $b|HV\rangle + c|VH\rangle$. By coherently superposing the above two processes, as shown in Fig. 2, the fully arbitrary pure two-qubit state $a|HH\rangle + b|HV\rangle + c|VH\rangle + d|VV\rangle$ can be created. The amplitude of each process, which is determined by the relative values of $\langle\psi_U|\psi_U\rangle$ and $\langle\psi_L|\psi_L\rangle$, can be adjusted by the transmission through the beam splitter. Moreover, coherent superposition can be achieved by balancing the two path lengths. Thus, by combining a well-balanced interferometer and the process of spontaneous downconversion we can realize arbitrary two-photon polarization *pure* states. In the next section we shall describe two schemes capable of producing arbitrary two-photon polarization *mixed* states.

## III. SCHEMES FOR ARBITRARY TWO-PHOTON POLARIZATION MIXED STATES

Any two-qubit mixed state can be canonically decomposed as follows [1]:

$$\rho = \sum_{i=1}^{4} \lambda_i |\psi_i\rangle\langle\psi_i|, \quad (9)$$

where $\{|\psi_i\rangle\}$ are orthonormal eigenstates of $\rho$. It is therefore natural to realize $\rho$ simply by mixing its eigenstates with probabilities proportional to their eigenvalues $\lambda_i$. As we can synthesize arbitrary pure states from one set of crystals, individual synthesis of each $|\psi_i\rangle$ is straightforward.

### A. Scheme I: Arbitrary two-qubit mixed states I

The first mixed-state scheme is shown in Fig. 3. We have four pairs of nonlinear crystals, each generating a pure state that, when propagating to the output, arrives as $|\psi_i\rangle$ [22]. There is an attenuator in front of each set of crystals (except the first set) such that the pump intensity $I_i$ going into the $i$-th set of crystals is proportional to $\lambda_i$ (arranged in decreasing order: $\lambda_1 \geq \lambda_2 \geq \lambda_3 \geq \lambda_4$).

| Schemes | Synthesizable states | CP | NLC | Other Optics | Advantages | Disadvantages |
|---|---|---|---|---|---|---|
| I : Fig. 3 | Arbitrary two qubits | 15 | 8 | 38 | Arbitrary states | 1. Birefringence of crystals causes additional rotations and possible decoherence<br>2. Requires precise spatial-mode alignment<br>3. Narrow opening angles of downconversion require long path difference for mixing<br>4. Potential loss of downconverted photons<br>5. Waveplate imperfection and wedges, esp. at early stages, cause beam deviation |
| II : Fig. 4 | Arbitrary two qubits | 15 | 2 | 48† | 1. Arbitrary states<br>2. Not lossy in downconversion<br>3. Only two crystals | 1. Requires interferometer stablization<br>2. Need to compensate reflection-induced transformations from mirrors<br>3. Variable beam splitters difficult to tune<br>4. Lossy in pump |
| III: Fig. 5 | MEMS Eq. (16), Werner (19), Collins-Gisin (23) and states (14) | $\geq 10$ | 2 | 10‡ | 1. Partially tested [6, 33, 34]<br>2. Minimal spatial-mode matching<br>3. Only two crystals | 1. Probably not arbitrary states<br>2. No complete theory for more than one decoherer per arm |
| IV: Fig. 6 | States from III, Bell-diagonal states (30) and states (26) | $\geq 12$ | 4 | 26 | More states than III | 1. Probably not arbitrary states<br>2. Birefringence of crystals causes additional rotations and possible decoherence<br>3. Requires precise spatial-mode alignment |

TABLE I: Comparison of the four mixed-state schemes. CP stands for controllable parameters (out of 15 in total). The nonlinear crystals (NLC) are used in the downconversion process. By "other resources", we include waveplates (where a general unitary requires, e.g., 1 half-waveplate and 2 quarter-waveplates, hence counted as 3 elements), mirrors, attenuators, prisms, and decoherers, and we assume that the pump is already polarized. The crystal and resource numbers given are sufficient to produce all states given in the final column. This resource accounting is intended to indicate the relative complexity of the various schemes; however, the numbers listed may be reduced for certain states, or possibly by using clever combinations of elements (e.g., reflections which modify polarization). †The resource number listed for Scheme II is several items lower than a direct counting from Fig. 4, which was shown for clarity with extra mirrors. ‡The resource number listed for Scheme III is counted without pump decoherence and with only a single stage of decoherence, and is thus less than a direct counting from Fig. 5, but is sufficient to synthesize the states listed.

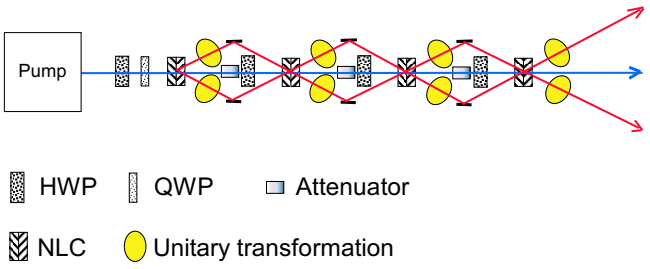


FIG. 3: (Color online) Scheme I employs four sets of nonlinear crystals. The two-photon state created at the $i$-th set of crystals is chosen such that it is the correct state $|\psi_i\rangle$ after propagation through the subsequent elements. The necessary local unitary transformations at each downconversion location can be readily calculated [22]. PBS: polarizing beam splitter; HWP: half-waveplate; QWP: quarter-waveplate; NLC: nonlinear crystals.

It is less favorable to attenuate the four downconversion pure states to tune the probabilities according to their eigenvalues, because direct attenuation of the downconversion photons would, in general, result in unpaired photons, i.e., one of the photons would be absorbed, but not the other [9].

For a pulsed pump, the mixing is incoherent, as the arrival time of the downconversion pair (relative to the pump pulse) can, in principle, reveal information on where the pair was generated. For a CW (continuous wave) pump, one can add a path delay (much greater than the pump coherence length [17]), to each pair such that pair-generation amplitudes at all sets of crystals are no longer coherent with one another. We can thus synthesize $\rho$ by incoherently mixing its eigenstates with appropriate weights. As the downconversion process is much more likely to produce one rather than multiple pairs [e.g., see Eq. (1)], multiple pairs can be ignored.

### B. Scheme II: Arbitrary two-qubit mixed states II

The interferometric scheme of Sec. II B can also be extended to create arbitrary mixed states. The full scheme is shown in Fig. 4. The coherent superposition method of Fig. 2 is used to create each of the four pure states $|\psi_i\rangle$ in the decomposition (9) and mix them incoherently in proportion to their eigenvalues $\lambda_i$, as in Scheme I. Arbitrary weights of mixing can be achieved by controlling the transmissions of the beam splitters. In order to mix the four parts incoherently, we first use timing information [23] such that the state of the pump is

$$|\psi_p\rangle = \sum_{i=1}^{4} (|\psi_{Ui}\rangle + |\psi_{Li}\rangle) \otimes |i\rangle_T. \tag{10}$$

Here, $|\psi_{Ui}\rangle$ and $|\psi_{Li}\rangle$ (both un-normalized) are the two parts of the pump state that will, ultimately, yield the corresponding pure state $|\psi_i\rangle$ [24]. The factors $|i\rangle_T$ ($i = 1, \ldots, 4$) encode timing information; there is no coherence between paths labelled by distinct values of $i$, i.e., $\langle i|j\rangle_T = \delta_{ij}$. For this absence of coherence to hold, the path-length difference between any two upper (or lower) unmatched paths must be greater than the pump coherence length [25]. As long as coherence is maintained for the corresponding pairs of states, $|\psi_{Ui}\rangle$ and $|\psi_{Li}\rangle$ (for $i = 1, \ldots, 4$), but the time differences for the $i$'s are distinguishable, the output state is the desired mixed state, once timing information is traced over, i.e., discarded [26]. Note, however, that there is no difference in *relative* timing between signal and idler photons. The timing information is coupled solely to the pump photons; because this timing information is traced over (ignored), downconversion produces an incoherent mixture of four two-photon states. Also note that with a CW pump, the only possibility to detect any coherence in the timing information would be to include similar unbalanced interferometers in the downconversion output.

The difference between the present scheme (II) and the previous one (I) is that for Scheme II each of the four pure states is created probabilistically in the same downconversion crystals, whereas for Scheme I each of the four pure states is created in downconversion crystals at distinct locations. Both schemes yield arbitrary two-qubit mixed states by incoherent temporal mixing.

## IV. RESOURCE-OPTIMIZED SCHEMES FOR MIXED STATES

In this section we describe two reduced schemes (III and IV) that provide practical ways to realize several important families of states that are currently of interest. Scheme III, whose feasibility has been demonstrated experimentally, emerges as an effort to reduce the number of downconversion crystals to two by sacrificing the generality of the synthesizable states. Scheme IV further extends the set of synthesizable states by employing two sets of crystals and the mixing technique introduced in Scheme I.

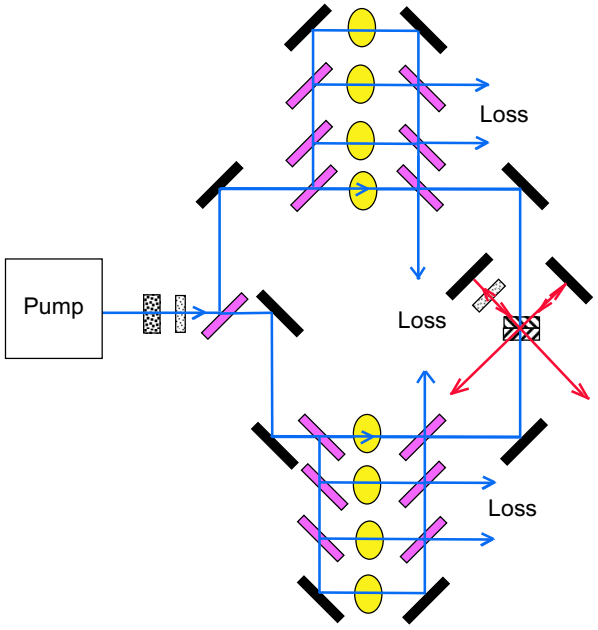


FIG. 4: (Color online) Arbitrary two-qubit mixed-state synthesis Scheme II. The transmission probabilities of the various beam splitters depend on the desired final state. The variable beam splitters immediate preceding the unitary rotations could also be realized by polarizing beam splitters with suitable polarization rotations before and after.

### A. Scheme III: Filling the tangle-entropy plane

Recall that Scheme I requires the use of, at most, four sets of SPDC crystals. Since fewer crystal sets would be more economical and likely easier to implement, we thus propose a modified scheme, which uses only one set of SPDC crystals but relies on "controlled" decoherence. Although we do not yet know whether this scheme can generate *arbitrary* two-qubit states, it can synthesize several important families of mixed states, including states with all physically allowed values of entanglement (characterized, e.g., by "tangle") and mixedness (characterized, e.g., by the linear entropy [27]).

We use thick birefringent crystals with thickness $L$ as "decoherers." Their effect on a polarization state of definite frequency $\omega$ is (see, e.g., [19, 28])

$$\mathrm{D}(L)|\chi_j\rangle \otimes |\omega\rangle = e^{in_j L\omega/c}|\chi_j\rangle \otimes |\omega\rangle, \tag{11}$$

where the optic axis is assumed to be along, say, $\chi_2$, i.e., the $V$ direction, and $n_j$ is the refractive index for the $j$-th polarization state. The decohering elements entangle the polarization and frequency degrees of freedom. In the output, only polarizations are detected, so we have to trace over the frequency degree of freedom in the joint pure state (of polarizations and frequencies). In general,

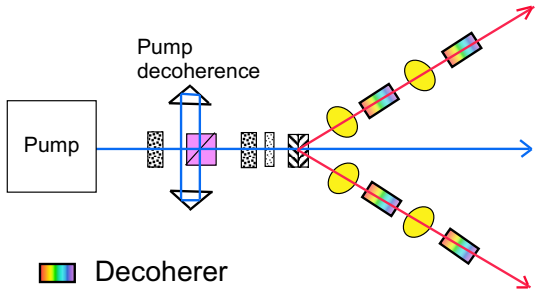


FIG. 5: (Color online) Scheme III employs decoherence. Downconversion photon pairs can be decohered, as well as pump photons. The decoherers are thick birefringent crystals, which separate different polarizations and decrease the coherence between them. Also shown is a possible decoherence on the pump beam: the vertical polarization component experiences an adjustable extra delay.

we are then left with a *mixed* two-photon polarization state. In the present scheme, we can have several decoherers in each arm, along with arbitrary unitary rotations between the decoherers (only two are shown in Fig. 5).

In addition to directly decohering the downconversion photons, one can also decohere the pump photons before downconversion, as indicated in Fig. 5. However, as mentioned previously, the pump typically has a much longer coherence length than the downconversion photons do, and hence may require much greater relative birefringent delays, e.g., unbalanced polarization interferometers, to achieve decoherence.

In the limit we are considering, i.e., $l_p \gg |\Delta n| L_{1/2} \gg l_{si}$ (where $\Delta n \equiv (n_{\rm V} - n_{\rm H})$, and $L_1$ and $L_2$ are respective thicknesses of the decoherers), decohering the pump in addition to the downconversion photons does not provide further control beyond simply decohering the downconversion photons. Hence, in the following analysis we shall not consider decohering the pump.

Consider a pure initial polarization state of downconversion pairs (7): $|\psi^{(1)}\rangle = a|HH\rangle + b|HV\rangle + c|VH\rangle + d|VV\rangle$ (which is created by the method described in Sec. II). After the decoherers $D(L_1)$ and $D(L_2)$, one in each of the two arms, the state is

$$|\psi\rangle = D(L_1) \otimes D(L_2) |\psi^{(1)}\rangle. \tag{12}$$

Tracing over the frequencies [29], the reduced density matrix for the polarization state is (with $\rho_\psi \equiv |\psi\rangle\langle\psi|$)

$$\rho = {\rm Tr}_\epsilon\, \rho_\psi = \int d\epsilon' \langle \frac{\omega}{2} + \epsilon', \frac{\omega}{2} - \epsilon' | \rho_\psi | \frac{\omega}{2} + \epsilon', \frac{\omega}{2} - \epsilon' \rangle. \tag{13}$$

In the limit $L_1, L_2 \gg c/(\delta_\epsilon |\Delta n|)$, where $\Delta n$ is assumed to be independent of $\epsilon$, the resulting polarization mixed state is (in the $\{|HH\rangle, |HV\rangle, |VH\rangle, |VV\rangle\}$ basis)

$$\begin{pmatrix} |a|^2 & 0 & 0 & fad^* \\ 0 & |b|^2 & 0 & 0 \\ 0 & 0 & |c|^2 & 0 \\ f^* a^* d & 0 & 0 & |d|^2 \end{pmatrix}, \tag{14}$$

where $f$ is a complex function of $L_1$ and $L_2$ whose exact form depends on $A_{si}(\epsilon)$. For $A_{si}(\epsilon)$ of gaussian form, as in Eq. (3), $f$ is given by

$$f = \exp\left( -\frac{1}{2} \left[ \frac{\Delta n (L_1 - L_2)}{c/\delta_\epsilon} \right]^2 \right) e^{-i \Delta n (L_1 + L_2) \omega / 2c}. \tag{15}$$

Note that $|f| \le 1$, with $|f| = 1$ for $L_1 = L_2$.

The family of two-qubit mixed states described by (14) turns out to be of the form hypothesized by Munro *et al.* [13] in their search for the maximally entangled mixed states (MEMS), which define the boundary of physically allowed states on the tangle-entropy plane [13, 30]. (The family (14) also contains other maximally entangled mixed states, corresponding to different charaterizations of entanglement and entropy [31].) Although states in this family actually fill the physically allowed region of the tangle-entropy plane, this does not mean that the family contains all two-qubit mixed states. In fact, the family (14) has only 4 independent real parameters excluding the phase of the off-diagonal element. By including the 6 additional real parameters coming from the two arbitrary local $SU(2)$ transformations, we can thus control 10 of the 15 real parameters associated with general two-qubit mixed states. This assumes a *single* decoherer in each arm. The full capability of Scheme III with an arbitrary number of decoherence stages is a difficult theoretical problem that requires further investigation.

Next we specifically describe how to generate maximally entangled mixed states, Werner states, and a particular class of mixed states recently discussed by Collins and Gisin [14]. The maximally entangled mixed states found by Munro *et al.* [13] are of the form

$$\rho_{\rm MEMS} = \begin{cases} \rho_{\rm I}(r), & \text{for } \frac{2}{3} \le r \le 1; \\ \rho_{\rm II}(r), & \text{for } 0 \le r \le \frac{2}{3}; \end{cases} \tag{16a}$$

$$\rho_{\rm I}(r) = \begin{pmatrix} \frac{r}{2} & 0 & 0 & \frac{r}{2} \\ 0 & 1-r & 0 & 0 \\ 0 & 0 & 0 & 0 \\ \frac{r}{2} & 0 & 0 & \frac{r}{2} \end{pmatrix}, \quad \rho_{\rm II}(r) = \begin{pmatrix} \frac{1}{3} & 0 & 0 & \frac{r}{2} \\ 0 & \frac{1}{3} & 0 & 0 \\ 0 & 0 & 0 & 0 \\ \frac{r}{2} & 0 & 0 & \frac{1}{3} \end{pmatrix}. \tag{16b}$$

Here, an irrelevant phase in the nonzero off-diagonal elements has been set to zero. For $\rho_{\rm I}(r)$, we only need to generate a pure state of the form

$$\sqrt{\frac{r}{2}} |HH\rangle + \sqrt{1-r} |HV\rangle + \sqrt{\frac{r}{2}} |VV\rangle, \tag{17}$$

followed by decoherers with thicknesses $L_1 = L_2$. For $\rho_{\rm II}(r)$, we start with

$$\sqrt{\frac{1}{3}} |HH\rangle + \sqrt{\frac{1}{3}} |HV\rangle + \sqrt{\frac{1}{3}} |VV\rangle, \tag{18}$$

followed by decoherers with thicknesses $L_1$ and $L_2$ such that $|f(L_1, L_2)| = 3r/2$ [6]. This requires either prior knowledge of $A_{si}(\epsilon)$ or the tuning of $(L_1 - L_2)$ so as

to obtain the correct reduction factor $|f|$. Similarly, to prepare the Werner states of the form

$$\rho_{\rm W}(r) \equiv r|\Phi^+\rangle\langle\Phi^+| + \frac{1-r}{4}\mathbb{1} = \begin{pmatrix} \frac{1+r}{4} & 0 & 0 & \frac{r}{2} \\ 0 & \frac{1-r}{4} & 0 & 0 \\ 0 & 0 & \frac{1-r}{4} & 0 \\ \frac{r}{2} & 0 & 0 & \frac{1+r}{4} \end{pmatrix}, \quad (19)$$

[with $|\Phi^+\rangle \equiv (|HH\rangle + |VV\rangle)/\sqrt{2}$], we start with the pure state

$$\sqrt{\frac{1+r}{4}}|HH\rangle + \sqrt{\frac{1-r}{4}}|HV\rangle + \sqrt{\frac{1-r}{4}}|VH\rangle + \sqrt{\frac{1+r}{4}}|VV\rangle, \quad (20)$$

and follow with decoherers with thicknesses $L_1$ and $L_2$ such that $|f(L_1, L_2)| = 2r/(1+r)$. Analogous procedures yield the other forms of the Werner states, i.e., with other maximally entangled components.

Using these methods, several maximally entangled mixed states and Werner states have been synthesized experimentally, with high fidelities [32] between the experimentally produced states and the theoretical target states. For example, the MEMS

$$\begin{pmatrix} \frac{1}{3} & 0 & 0 & \frac{1}{3} \\ 0 & \frac{1}{3} & 0 & 0 \\ 0 & 0 & 0 & 0 \\ \frac{1}{3} & 0 & 0 & \frac{1}{3} \end{pmatrix} \quad (21)$$

was used to investigate entanglement purification protocols [6], and the separable Werner state

$$\begin{pmatrix} \frac{1}{3} & 0 & 0 & \frac{1}{6} \\ 0 & \frac{1}{6} & 0 & 0 \\ 0 & 0 & \frac{1}{6} & 0 \\ \frac{1}{6} & 0 & 0 & \frac{1}{3} \end{pmatrix} \quad (22)$$

was used to perform ancilla-assisted process tomography without entanglement [33].

Next, we turn to the Collins-Gisin states, particular mixtures of two pure states:

$$\rho_{\rm CG}(\lambda, \theta) \equiv \lambda|\psi_\theta\rangle\langle\psi_\theta| + (1-\lambda)|HV\rangle\langle HV| = \begin{pmatrix} \lambda\cos^2\theta & 0 & 0 & \lambda\cos\theta\sin\theta \\ 0 & (1-\lambda) & 0 & 0 \\ 0 & 0 & 0 & 0 \\ \lambda\cos\theta\sin\theta & 0 & 0 & \lambda\sin^2\theta \end{pmatrix}, \quad (23)$$

where $|\psi_\theta\rangle \equiv \cos\theta|HH\rangle + \sin\theta|VV\rangle$. Collins and Gisin reported a Bell-like inequality (which they call I3322) that is *inequivalent* to the usual CHSH-Bell inequality [35], in that there are states that do not violate CHSH but *do* violate I3322 [14]. For example, the family of states $\rho_{\rm CG}(\lambda, \theta)$ exhibit this behavior for certain ranges of $\lambda$ and $\theta$ where no violations of CHSH occur. How can we create these Collins-Gisin states? In light of the above examples of MEMS and Werner states, we see that we only need to generate a pure state of the form

$$\sqrt{\lambda}\cos\theta\,|HH\rangle + \sqrt{1-\lambda}\,|HV\rangle + \sqrt{\lambda}\sin\theta\,|VV\rangle, \quad (24)$$

followed by a decoherence with $L_1 = L_2$. Such states have been experimentally realized and used to study various tests for entanglement and nonlocality [34].

States described by Eq. (14) (plus those derived from them by local unitary transformations) are not the most general form that Scheme II can achieve. For example, if, via downconversion, we prepare the pure state $|\Psi^+\rangle \equiv (|HV\rangle + |VH\rangle)/\sqrt{2}$, apply decoherers of common thickness $L$ ($\gg l_{si}$) in both arms, and then rotate each photon polarization by 45°, followed by a second set of decoherers with the same thicknesses, we would generate a mixed state of the form

$$\begin{pmatrix} \frac{1}{4} & 0 & 0 & \frac{1}{4} \\ 0 & \frac{1}{4} & \frac{1}{8} & 0 \\ 0 & \frac{1}{8} & \frac{1}{4} & 0 \\ \frac{1}{4} & 0 & 0 & \frac{1}{4} \end{pmatrix}, \quad (25)$$

up to some irrelevant phases. This state does not belong to the family (14), obtained with only one stage of decoherence, suggesting that using multiple decoherences may enable control over *more* than the 10 independent parameters allowed by a single decoherence. Further theoretical investigation is needed to determine the most general states obtainable.

### B. Scheme IV: A hybrid technique

From Scheme I it appears that one needs four sets of nonlinear crystals in order to synthesize fully general rank-four mixed states, whereas from Scheme III one can create rank-four mixed states of the restricted form (14) (up to local unitary transformations) with a single set of crystals. As we now discuss, by using a hybrid scheme one can, with only two sets (or in some cases, even just a single set) of crystals, generate a larger class of rank-four mixed states.

The idea is as follows. Suppose that the state $\rho$ can be decomposed into

$$\rho = p\,\sigma + (1-p)|\psi\rangle\langle\psi|. \quad (26)$$

If the mixed state $\sigma$ can be created by Scheme III [e.g., states in Eq. 14], we can then mix, with appropriate weights, $\sigma$ (as created from a first set of crystals) with the pure state $|\psi\rangle\langle\psi|$ (from a second set), and thus obtain $\rho$ [36]; see Fig. 6a. Although any two-qubit mixed state always allows a decomposition into a mixed state plus a pure part [37], it remains an open question whether there always exists a decomposition for which the mixed-state part is achievable by Scheme III. Nevertheless, this

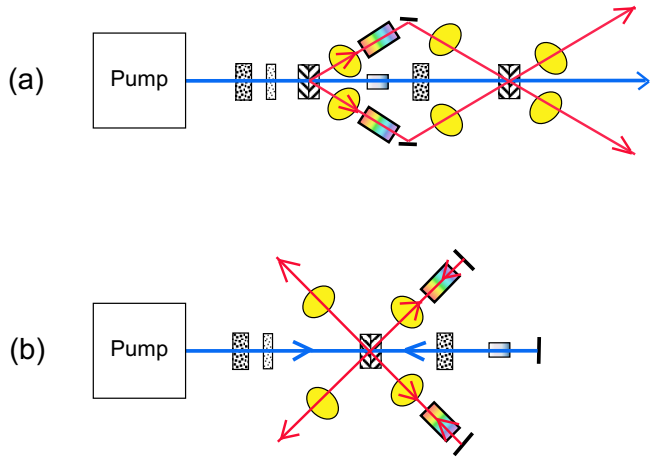


FIG. 6: (Color online) Scheme IV is a hybrid technique. (a) Mixing a pure state with a mixed state. The local unitary transformations immediately after the decoherers are used to pre-compensate the effect of local unitary transformations used afterward to rotate the pure part, and also to undo any effects of passing through the nonlinear crystals (c.f. Fig. 3). (b) A reduced setup of the method in (a), using only one set of nonlinear crystals, and retro-reflecting the pump back through the nonlinear crystals and the first photon pair back into the spatial modes of the second pair. Setup (b) is less general than (a), as the pure-state part cannot be chosen arbitrarily.

hybrid scheme can obviously generate more states than Scheme III alone, since adding the pure part adds more degrees of freedom.

We can make a simple reckoning of the number of parameters of the achievable density matrices independently controllable. Suppose we restrict the mixed-state part $\sigma$ to be produced by Scheme III with only one stage of decoherence, i.e., $\sigma$ is of the form (14) with all parameters real. Recall that a general two-qubit pure state can be expressed as

$$|\psi\rangle = U_A \otimes U_B\big(\sqrt{\lambda}|HV\rangle + \sqrt{1-\lambda}|VH\rangle\big), \qquad (27)$$

where $U_A$ and $U_B$ are local unitary transformations, and $\sqrt{\lambda}$ and $\sqrt{1-\lambda}$ are Schmidt coefficients. Expressed in the basis in which the pure state $|\psi\rangle$ is Schmidt decomposed, the mixed state $p\,\sigma + (1-p)|\psi\rangle\langle\psi|$ appears as

$$p\,U_A^\dagger \otimes U_B^\dagger \begin{pmatrix} a^2 & 0 & 0 & fad \\ 0 & b^2 & 0 & 0 \\ 0 & 0 & c^2 & 0 \\ fad & 0 & 0 & d^2 \end{pmatrix} U_A \otimes U_B$$
$$+(1-p)\begin{pmatrix} 0 & 0 & 0 & 0 \\ 0 & \lambda & \sqrt{\lambda(1-\lambda)} & 0 \\ 0 & \sqrt{\lambda(1-\lambda)} & 1-\lambda & 0 \\ 0 & 0 & 0 & 0 \end{pmatrix}. \qquad (28)$$

For fixed $U_A$ and $U_B$, this gives, in general, 6 independent parameters $\{a, b, c, f, p, \lambda\}$ [noting that $d$ is not independent of $\{a, b, c\}$]. Barring some coincidence that, for different pairs of $\{a, b, c, d, f\}$ and $\{U_A, U_B\}$, gives the same mixed part, we have in total 12 independent parameters, after adding 6 from the local unitaries [38].

One important family of states that this scheme can synthesize (and which cannot be generated via Scheme III with only one stage of decoherence) are the arbitrary Bell-diagonal mixed states [3]:

$$\rho_B \equiv \lambda_1|\Phi^+\rangle\langle\Phi^+| + \lambda_2|\Phi^-\rangle\langle\Phi^-| + \lambda_3|\Psi^+\rangle\langle\Psi^+| + \lambda_4|\Psi^-\rangle\langle\Psi^-|. \qquad (29)$$

Expressed in the $\{|HH\rangle, |HV\rangle, |VH\rangle, |VV\rangle\}$ basis

$$\rho_B = \frac{1}{2}\begin{pmatrix} \lambda_1+\lambda_2 & 0 & 0 & \lambda_1-\lambda_2 \\ 0 & \lambda_3+\lambda_4 & \lambda_3-\lambda_4 & 0 \\ 0 & \lambda_3-\lambda_4 & \lambda_3+\lambda_4 & 0 \\ \lambda_1-\lambda_2 & 0 & 0 & \lambda_1+\lambda_2 \end{pmatrix}. \qquad (30)$$

Assuming that $|\lambda_3 - \lambda_4| \le 1/2$ (otherwise $|\lambda_1 - \lambda_2| \le 1/2$), $\rho_B$ can also be decomposed as

$$\rho_{\rm B} = (1 - |\lambda_3 - \lambda_4|)\rho_1 + |\lambda_3 - \lambda_4|\,|\Psi\rangle\langle\Psi|, \qquad (31)$$

where $(1 - |\lambda_3 - \lambda_4|)\rho_1$ is

$$\frac{1}{2}\begin{pmatrix} \lambda_1{+}\lambda_2 & 0 & 0 & \lambda_1{-}\lambda_2 \\ 0 & \lambda_3{+}\lambda_4{-}|\lambda_3{-}\lambda_4| & 0 & 0 \\ 0 & 0 & \lambda_3{+}\lambda_4{-}|\lambda_3{-}\lambda_4| & 0 \\ \lambda_1{-}\lambda_2 & 0 & 0 & \lambda_1{+}\lambda_2 \end{pmatrix} \qquad (32a)$$

and the pure-state part is a Bell state

$$|\Psi\rangle = \frac{1}{\sqrt{2}}\big(|HV\rangle + \mathrm{sgn}(\lambda_3{-}\lambda_4)|VH\rangle\big). \qquad (32b)$$

Here $\mathrm{sgn}(x)$ is the sign function, which gives a factor of $\pm 1$, depending on the sign of $x$. It is clear that $\rho_1$ belongs to the family of states (14), and hence can be synthesized by Scheme III with one stage of decoherence; on the other hand, $|\Psi\rangle$ is a Bell state, which can be easily generated. Furthermore, the weight of $\rho_1$ is not less than that of $|\Psi\rangle\langle\Psi|$, so there is no need to attenuate the intensity of the mixed part [36]. Therefore, Scheme IV can synthesize *any* Bell-diagonal state $\rho_{\rm B}$. The Bell-diagonal states, if entangled, can be readily distilled via the BBPSSW scheme [3, 39] into states with more entanglement. They also have the property that, for a given set of eigenvalues, they achieve the maximal violation of the CHSH-Bell inequality [40].

For certain states this hybrid scheme can also be implemented via a single set of crystals, by reflecting the source and the downconversion pair back through the crystals with a mirror; see Fig. 6b. However, in this case, the pure-state part cannot be arbitrarily chosen, as the local unitary transformations needed to create the mixed part $\sigma$ and the pure part $|\Psi\rangle$ are no longer independent. The mixed part $\sigma$ is obtained via locally rotating $\alpha_1|HH\rangle + \beta_1|VV\rangle$ by $\hat{U}_A \otimes \hat{U}_B$, followed by

a decoherence. As the photons reflect back from the mirrors, they experience again the same local unitary transformation $\hat{U}_A \otimes \hat{U}_B$. The local unitary transformation at the output port is then chosen to eliminate this additional effect (by choosing the inverse of this transformation), thereby fixing $\sigma$ to be of the form (14); the pure state part is consequently limited to the form $|\psi\rangle = \hat{U}_A^{-1} \otimes \hat{U}_B^{-1} (\alpha_2|HH\rangle + \beta_2|VV\rangle)$. Any further local unitary transformation will rotate $\sigma$ and $|\psi\rangle$ together and cannot change this relative relation.

## V. CONCLUDING REMARKS

We have described two approaches for synthesizing arbitary two-qubit pure states. Based on these, we have developed four schemes for synthesizing two-qubit photon polarization *mixed* states. Scheme I (Fig. 3) requires several sets of downconversion crystals to create arbitrary two-qubit mixed states. It would be desirable to experimentally synthesize rank-two mixed states using this scheme, in order to give a proof-of-principle demonstration. Scheme II (Fig. 4) employs temporal mixing to achieve decoherence. It offers a second way to realize arbitrary two-photon polarization mixed states, but—significantly—requires only one set of downconversion crystals, at the cost of requiring several rather large, phase-stabilized interferometers. Scheme III (Fig. 5) provides control over at least 10 of the independent real parameters of two-qubit mixed states, and gives access to all physically allowed values of entanglement and entropy. Furthermore, this scheme has been experimentally implemented to synthesize several interesting families of mixed states, such as Werner states, maximally entangled mixed states, and Collins-Gisin states [6, 33, 34]. The fourth scheme (Fig. 6), extends the range of Scheme III (providing control over 12 mixed-state parameters). In particular, this scheme can be used to produce arbitrary Bell-diagonal states, which are of interest, e.g., in entanglement distillation [3, 39] and maximal violations of Bell inequalities [40]. Although the full capabilities of Schemes III and IV are not yet entirely clear, our analysis shows that these two schemes provide practical methods for creating quite general mixed states, many of which were previously not accessible experimentally. The four mixed-state schemes are summarized and compared in Table I, including the respective resources, advantages and disadvantages for implementation.

Once one has well-controlled arbitrary two-qubit sources, they will be usable for many quantum information processing applications, such as testing methods of entanglement distillation [3, 6, 39, 41], investigating quantum process tomography [33, 42], characterizing quantum gates [43], testing violations of Bell-type inequalities [8, 15, 35, 40] by mixed states (including a relevant two-qubit Bell inequality [14] that is inequivalent to the CHSH inequality), and exploring the vast, previously inaccessible territory of Hilbert space.

**Acknowledgments**

The authors would like to acknowledge useful discussions with Bill Munro and Sam Braunstein. This work was supported by NSF Award No. EIA01-21568, ARDA, the DCI Postdoctoral Research Fellowship Program, and by the MURI Center for Photonic Quantum Information Systems (ARO/ARDA program DAAD19-03-1-0199) .

## APPENDIX A: CREATING ARBITRARY PURE STATES

In this appendix we explain how to create an arbitrary two-qubit pure state, characterized by $\{a, b, c, d\}$ of Eq. (7). This amounts to establishing adequate local unitary transformations ($U_A$ and $U_B$) and post-SPDC pure states Eq. (5) of the form that SPDC naturally yields. For convenience, we exchange the coefficients $\cos\theta$ for $\alpha$ and $e^{i\phi}\sin\theta$ for $\beta$.

To find the appropriate settings and local unitary transformations, we need to solve

$$\begin{aligned} U_A \otimes U_B(\alpha|HH\rangle + \beta|VV\rangle) = \\ a|HH\rangle + b|HV\rangle + c|VH\rangle + d|VV\rangle, \end{aligned} \tag{A1}$$

for $\{U_A, U_B, \alpha, \beta\}$, given $\{a, b, c, d\}$ that are properly normalized. This equation can be solved either by Schmidt decomposition or by direct algebraic manipulation. However, the solution is not unique.

When $ad - bc = 0$, the state to synthesize is a product state, which can be created from an initial state $|HH\rangle$ followed by independent local rotations (see, e.g., Ref. [19]). For

$$ad - bc \neq 0, \qquad |ad - bc| \neq 1/2, \tag{A2}$$

i.e., the case of non-maximally entangled pure states, one possible solution is

$$\alpha = \sqrt{1 - \sqrt{1 - 4|ad - bc|^2}}/\sqrt{2}, \tag{A3a}$$

$$\beta = (ad - bc)/\alpha, \tag{A3b}$$

$$U_A = \begin{pmatrix} u_1 & v_1 \\ -v_1^* & u_1^* \end{pmatrix}, \quad U_B = \begin{pmatrix} u_2 & v_2 \\ -v_2^* & u_2^* \end{pmatrix}, \tag{A3c}$$

where

$$u_1 \equiv |z_1|/\sqrt{|z_1|^2 + |z_3|^2}, \quad v_1 \equiv z_3 u_1^*/z_1^*, \tag{A4a}$$

$$u_2 \equiv z_3^*/(z_1 z_3 + z_2 z4), \quad v_2 \equiv z_2/(z_1 z_3 + z_2 z_4), \tag{A4b}$$

with $z_1, z_2, z_3, z_4$ defined via

$$z_1 \equiv (\ a\alpha^* - d^*\beta)/(|\alpha|^2 - |\beta|^2), \tag{A5a}$$

$$z_2 \equiv (\ d^*\alpha - a\beta^*)/(|\alpha|^2 - |\beta|^2), \tag{A5b}$$

$$z_3 \equiv (-c^*\alpha - b\beta^*)/(|\alpha|^2 - |\beta|^2), \tag{A5c}$$

$$z_4 \equiv (-b\alpha^* - c^*\beta)/(|\alpha|^2 - |\beta|^2). \tag{A5d}$$

When $|ad-bc|=1/2$ there are three possible cases:
(i) $b=c=0$ and $|a|=|d|=1/\sqrt{2}$;
(ii) $a=d=0$ and $|b|=|c|=1/\sqrt{2}$;
(iii) $a,b,c,d\neq 0$, $|a|=|d|$, $|b|=|c|$.
Case (i) is already the form we seek. In case (ii), an exchange $H\leftrightarrow V$ (e.g., by a half-waveplate) will do. In case (iii), one possible solution is

$$e^{i\gamma} \equiv a/d^* = -b/c^*, \tag{A6a}$$

$$(\alpha,\beta) = (e^{i\gamma},1)/\sqrt{2}, \tag{A6b}$$

$$U_A = \frac{1}{\sqrt{2}}\begin{pmatrix} 1 & e^{i\gamma} \\ -e^{-i\gamma} & 1 \end{pmatrix}, \tag{A6c}$$

$$U_B = \begin{pmatrix} d^*-c & d^*+c \\ -d-c^* & d-c^* \end{pmatrix}. \tag{A6d}$$

In fact, this last case includes the previous two cases, if one interprets the phase in Eq. (A6a) to be the appropriate ratio of the nonzero coefficients. We remark that the solution presented above is not unique, and that experimentally one would implement the one that is most convenient.


[1] See, e.g., M. Nielsen and I. Chuang, *Quantum Computation and Quantum Information* (Cambridge University Press, Cambridge 2000).
[2] P. W. Shor, Phys. Rev. A **52**, 2493 (1995).
[3] C. H. Bennett, G. Brassard, S. Popescu, B. Schumacher, J. A. Smolin, and W. K. Wootters, Phys. Rev. Lett. **76**, 722 (1996).
[4] I. L. Chuang, N. Gershenfeld, and M. Kubinec, Phys. Rev. Lett. **80**, 3408 (1998).
[5] A. G. White, D. F. V. James, W. J. Munro, and P. G. Kwiat, Phys. Rev. A. **65**, 012301 (2001).
[6] N. A. Peters et al., Phys. Rev. Lett. **92**, 133601 (2004). P. G. Kwiat et al., quant-ph/0303040.
[7] Y. S. Zhang, Y. F. Huang, C. F. Li, G. C. Guo, Phys. Rev. A **66**, 062315 (2002).
[8] M. Barbieri, F. De Martini, G. Di Nepi, P. Mataloni, Phys. Rev. Lett. **92**, 177901 (2004).
[9] At the time of submission, we learned of a related work by C. Zhang, Phys. Rev. A **69**, 014304 (2004), which uses downconversion, beam splitters, and single-mode fibers to accomplish arbitrary two-photon polarization mixed states. However, that scheme requires coupling of four spatial modes into a single-mode fiber. This is necessarily a nonunitary (and very lossy) process, so that the desired two-qubit states are only generated for a small fraction, since the post-selected ensemble is much smaller (by a factor of 16) than the ensemble of emitted pairs. The methods described in the present paper do not require such postselection.
[10] A purification of a mixed state is a hypothetical extension of the state into an enlarged Hilbert space formed by adding ancillas such that the extended state is a pure state in the enlarged space. Upon tracing over the ancillas, the state reduces to the original mixed state [1]. As a two-qubit state $\rho$ can always be decomposed in the canonical form in Eq. (9), an immediate example of its purification is $|\psi_P\rangle \equiv \sum_{i=1}^{4}\sqrt{\lambda_i}|\psi_i\rangle\otimes|i\rangle_a$, where $|1\rangle_a, |2\rangle_a, |3\rangle_a$, and $|4\rangle_a$ are ancilla states. For example, the $|i\rangle_a$ could be encoded in the two-photon polarization states of two additional photons: $|HH\rangle, |HV\rangle, |VH\rangle$, and $|VV\rangle$. If there exist efficient CNOT gates, creating the four-photon pure state $|\psi_P\rangle$ is a straightforward procedure of unitary operations. However, such efficient entangling gates for photon polarizations are not yet available. See also [11].
[11] However, recently non-deterministic CNOT gates for photon polarizations have been achieved using a post-selection method. See, e.g., T. B. Pittman, M. J. Fitch, B. C. Jacobs, and J. D. Franson, Phys. Rev. A **68**, 032316 (2003), J. L. O'Brien, G. J. Pryde, A. G. White, T. C. Ralph, D. Branning, Nature **426**, 264 (2003), and K. Sanaka, T. Jennewein, J.-W. Pan, K. Resch, and A. Zeilinger, Phys. Rev. Lett. **92**, 017902 (2004).
[12] R. F. Werner, Phys. Rev. A **40**, 4277 (1989).
[13] W. J. Munro, D. F. V. James, A. G. White, and P. G. Kwiat, Phys. Rev. A. **64**, 030302 (2001).
[14] D. Collins and N. Gisin, J. Phys. A: Math. Gen. **37**, 1775 (2004).
[15] P. G. Kwiat, E. Waks, A. G. White, I. Appelbaum, and P. H. Eberhard, Phys. Rev. A **60**, R773 (1999); A. G. White, D. F. V. James, P. H. Eberhard, and P. G. Kwiat, Phys. Rev. Lett. **83**, 3103 (1999).
[16] Z. Y. Ou, L. J. Wang, X. Y. Zou, and L. Mandel, Phys. Rev. A **41**, 1597 (1990).
[17] Typical lasers have coherence lengths between 1cm and 1m. Practically, downconversion coherence lengths are selected experimentally with narrow-bandpass ($\Delta\lambda$) interference filters and are given by $l_{si}\approx\lambda^2/\Delta\lambda$. For example, for 700 nm photons with 1 nm (5 nm) bandpass interference filters, the coherence length is roughly 500 $\mu$m (100 $\mu$m).
[18] As the opening angle in our downconversion is small and fixed at $\sim 3^\circ$, we have ignored the effect of variation in polarization direction as the scattering angle varies, the variation being dramatic at large angles. For discussions of this effect, see A. Migdall, Journal of the Optical Society of America B-Optical Physics **14**, 1093 (1997).
[19] N. Peters, J. Altepeter, E. Jeffrey, D. Branning, and P. Kwiat, Quantum Inf. Comput. **3**, 503 (2003).
[20] A waveplate is a birefringent material that has a fixed retardance of light between two polarizations, one parallel to the optical axis (usually called extraordinary, with corresponding index of refraction $n_e$), the other perpendicular (usually called ordinary, with index of refraction $n_o$). The retardance between the extraordinary and ordinary

light is defined as $\delta \equiv (n_e - n_o)L/\lambda$, where $L$ is the thickness of the crystal and $\lambda$ is the wavelength of light. Retardances that differ by an integer give a phase of multiples of $2\pi$. A true zero-order waveplate has retardance usually less than one, but is usually too thin for practical use. A multi-order waveplate has $\delta > 1$, and is therefore more sensitive to variations in the wavelength. A compound zero-order waveplate is composed of two multi-order waveplates with their optic axes orthogonal to each other such that the net retardance is less than 1. Hence, compound zero-order waveplates are less sensitive to wavelength than are multi-order waveplates (but *more* sensitive to alignment and beam non-collimation). See, e.g., applications notes on "Sources of error in retarders and waveplates," http://www.meadowlark.com/AppNotes/, Meadowlark Optics, Inc. (2003).

[21] T. J. Herzog, P. G. Kwiat, H. Weinfurter, and A. Zeilinger, Phys. Rev. Lett. **75**, 3034 (1995).

[22] The local unitary transformations at each stage can be calculated backwards, starting with those at the fourth set of crystals. The unitary transformations caused by the nonlinear crystals themselves can be compensated by modifying the local unitary transformations. Decoherence effects arising from waveplates and crystals are assumed to be negligible.

[23] J. Brendel, N. Gisin, W. Tittel, and H. Zbinden, Phys. Rev. Lett. **82**, 2594 (1999).

[24] The probabilities (i.e., the eigenvalues or, equivalently, the relative intensities) can be included in the normalization of the states $|\psi_{Ui}\rangle$ and $|\psi_{Li}\rangle$. Note that the actual pump state before downconversion includes some amplitudes that will inevitably be lost (out of unused beamsplitter ports, as indicated by the subscripts "loss"), so it will be of the form

$$|\psi_p\rangle = \sum_{i=1}^{4}(|\psi_{Ui}\rangle + |\psi_{Li}\rangle) \otimes |i\rangle_T \ + |\psi_{U,\mathrm{loss}}\rangle + |\psi_{L,\mathrm{loss}}\rangle.$$

This loss is of no consequence in practice, as the pump contains large numbers of photons, and the creation of a particular two-photon state will be post-selected by coincidence counts.

[25] For example, for a pump with a 10 cm coherence length, a path-length difference of 30 cm is sufficient to eliminate coherence to 1%, assuming the dependence $\exp[-(\Delta L/l_p)^2/2]$.

[26] One can argue that the state (10) is a purification of the mixed state, with the "ancillas" being the timing information; see also remarks in [10].

[27] Tangle is a measure of entanglement associated with entanglement of formation; see W. K. Wootters, Phys. Rev. Lett. **80**, 2245 (1998). The linear entropy for a two-qubit state $\rho$ is defined as $(4/3)(1 - \mathrm{Tr}\rho^2)$; see Ref. [13].

[28] A. J. Berglund, Dartmouth College B.A. thesis (2000); also in quant-ph/0010001.

[29] In general, one has to integrate over the two independent frequencies $\omega_i$ and $\omega_s$ of the idler and singal photons. However, as we are considering the limit in which the pump is treated as monochromatic, there is a constraint: $\omega_i + \omega_s = \omega$. Hence, the only independent variable to integrate over is the deviation $\epsilon$ from half of the pump frequency (for either idler or signal photon).

[30] A. G. White, D. F. V. James, W. J. Munro, and P. G. Kwiat Phys. Rev. A **65**, 012301 (2002).

[31] T.-C. Wei et al., Phys. Rev. A **67**, 022110 (2003).

[32] The fidelity is a measure of how close two states are: $F(\rho,\sigma) \equiv \left(\mathrm{Tr}\sqrt{\sqrt{\rho}\,\sigma\sqrt{\rho}}\right)^2$ is the definition given in R. Jozsa, J. Mod. Optics **41**, 2315 (1994), whereas $F(\rho,\sigma) \equiv \mathrm{Tr}\sqrt{\sqrt{\rho}\,\sigma\sqrt{\rho}}$ is the definition in Ref. [1].

[33] J. B. Altepeter et al., Phys. Rev. Lett. **90**, 193601 (2003).

[34] J. B. Altepeter et al., submitted to Phys. Rev. Lett. (2004).

[35] J. F. Clauser, M. A. Horne, A. Shimony, and R. A. Holt, Phys. Rev. Lett. **23**, 880 (1969).

[36] If $p \leq 1/2$, we may need to attenuate the intensity of the photon pair from the first set of crystals. Alternatively, to losslessly prepare the state, we can switch the order of the setup such that the pure state $|\psi\rangle$ is created in the first set of crystals, and the mixed state $\sigma$ is created in the second. However, the photons from the former will then have to be pre-compensated to eliminate the effect of the subsequent decoherence. This can be done by using the same decoherers but with their optic axes rotated by $90^\circ$.

[37] M. Lewenstein and A. Sanpera, Phys. Rev. Lett. **80**, 2261 (1998).

[38] If the pump is decohered before the second set of crystals, the downconversion pair will be in a mixed state (up to local unitaries)

$$\begin{pmatrix} 0 & 0 & 0 & 0 \\ 0 & \lambda & g\sqrt{\lambda(1-\lambda)} & 0 \\ 0 & g^*\sqrt{\lambda(1-\lambda)} & 1-\lambda & 0 \\ 0 & 0 & 0 & 0 \end{pmatrix},$$

where $g$ represents the degree of decoherence of the pump (c.f., $f$ in Eq. (14)). It is not clear whether this additional "knob" boosts the number of independent controlled parameters from 12 to 13.

[39] J. W. Pan, C. Simon, Č. Brukner, and A. Zeilinger, Nature **410**, 1067 (2001); J. W. Pan, S. Gasparoni, R. Ursin, G. Weihs, and A. Zeilinger, Nature **423**, 417 (2003).

[40] F. Verstraete and M. M. Wolf, Phys. Rev. Lett. **89**, 170401 (2002).

[41] T. Yamamoto, M. Koashi, S. K. Özdemir, and N. Imoto, Nature **421**, 343 (2003).

[42] F. De Martini, A. Mazzei, M. Ricci, and G. M. D'Ariano, Phys. Rev. A **67**, 062307 (2003).

[43] A. G. White et al., quant-ph/0308115.